Proceedings of ERAD 2006

# Microphysical quantitative study of MAP-IOP3 through comparisons between radar observations and numerical simulations

**Olivier Pujol[1], Franck Lascaux[1] and Jean-François Georgis[1]**

[1] Université Paul Sabatier, Laboratoire d'aérologie, Toulouse (France).

## 1 Introduction

In this work, the microphysical processes involved in MAP-IOP3 (25-26/09/1999) precipitation development are identified and quantified using hydrometeor mixing ratio $r$ (g kg$^{-1}$) and budget computations from the Meso-NH model. This one was already used to study various IOP (Lascaux et al. 2006) and succeeded in reproducing precipitation characteristics (localization, intensity). Using polarimetric radar data and a fuzzy logic algorithm, Pujol et al. (2005) deduced qualitative conclusions on the IOP3 precipitation microphysical characteristics, but, broadly speaking, radars do not permit to make calculations as numerical model can do. Herein, the conclusions of Pujol et al. (2005) are completed by receiving a quantitative numerical support from Meso-NH.

In section 2, we briefly describe the context of the IOP3 and the numerical setup. Section 3 deals with microphysical temporal mean results. First, the observed and computed hydrometeor vertical structures of the IOP3 orographic precipitating system are presented and compared; second, the microphysical mechanisms involved in precipitation growth are quantified. Section 4 is the concluding one.

## 2 Brief recall of the IOP3 context and numerical setup

### 2.1 Context of the IOP3 (25/09/1999)

During IOP3, a trough located over North Atlantic generated a southwesterly flow over the Mediterranean Sea towards the Alps. In addition, airflow was warm, with a 0°C isotherm at about 3.5 km altitude, and potentially unstable at low level. Conditions were thus propitious for precipitation over the Alps. Indeed, they occurred at the end of the afternoon, with a very active phase from about 1700 to 2000 UTC, over the Lago Maggiore Target Area (LMTA). Data were retrieved by three ground-based Doppler radars (the Swiss one at Monte-Lema, the US SPOL polarimetric one, and the French one Ronsard) and interpolated on a 80 km square domain centered on the Lago Maggiore (Italy) at (46.10 N, 8.75 E), with a horizontal and vertical resolution of 1 and 0.5 km, respectively (Fig. 1). Many further details about radar observations and data processing are available in Pujol et al. (2005).

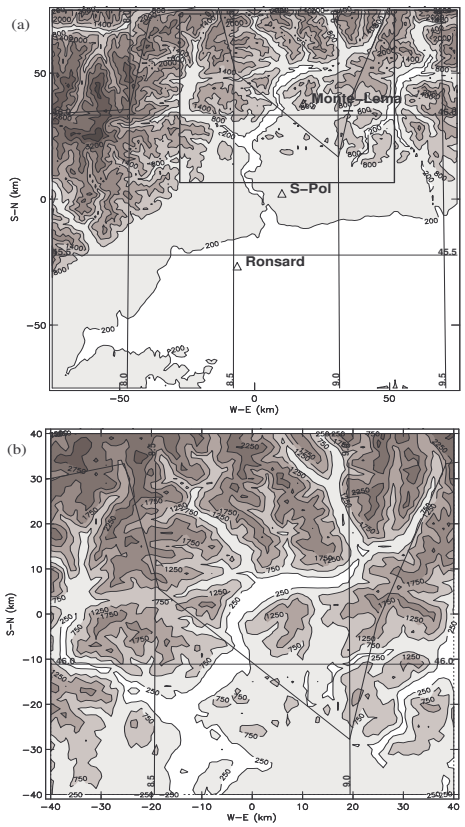


**Fig. 1.** (a) Triple radar network and underlying terrain in the Lago Maggiore Target Area during MAP (contours every 600 m). (b) Domain of Doppler-derived wind and precipitation contours every 500 m). This domain corresponds to the budget box used in the microphysical budget computations.

*Correspondence to:* Olivier Pujol.

pujo@aero.obs-mip.fr

Microphysical numerical simulations were performed with the non hydrostatic mesoscale model Meso-NH on the same domain with the finer horizontal resolution of 2 km, and using the explicit bulk microphysical scheme ICE4 which predicts the evolution of the mixing ratios of seven water species: vapor, cloud droplets (C), raindrops (R), ice crystals (I), snow (S), graupel (G) and hail (H). Further details about Meso-NH can be found in Lascaux et al. (2006) and in the Meso-NH documentation available on the website (http://www.aero.obs-mip.fr/mesonh). For the simulations, initial and boundary conditions were performed by the MAP-ECMWF re-analyses (Keil and Cardinali 2004), initial time was 25/09/1999 at 1200 UTC and integration was over 36 hours.

## 3 Temporal mean microphysical characteristics

To compare correctly radar observations and Meso-NH simulations, a vocabulary convention about which hydrometeor classes to consider is required. Precisely, we have to situate the classification used by Pujol et al. (2005) to make it consistent with the Meso-NH one. Fuzzy logic hydrometeor discrimination by Pujol et al. (2005) was made by considering seven classes: light, medium and heavy rain (LR, MR, HR respectively), dry and wet snow (DS and WS), ice crystals (IC) and graupel-hail mixture (GH). In this study, it is natural to merge LR, MR and HR in R; for iced particles, DS and IC are respectively identified with S and I. For mixed phase, finding equivalence is not so easy: in the fuzzy logic algorithm G and H was not differentiated, and WS is an extra category; besides, this last one can be considered as included in G for Meso-NH. The two studies are thus complementary for hydrometeor in mixed phase. Further, C is provided by the model and not by radars due to their small diameter and so their low reflectivity.

### 3.1 Hydrometeor vertical profile (Fig. 2)

Mean number of radar grid points associated with a given observed hydrometeor class and mean mixing ratio $r$ of each hydrometeor model output are displayed in figure 2a and 2b, respectively. In spite of some slight differences, observations and simulations are in agreement by presenting similar hydrometeor vertical profiles indicative of convective microphysical mechanisms:

- Solid phase (S and I): they present two relative maximum coordinates ($r_{max}$ (g kg$^{-1}$); $z$ (km)) - $z$ being the altitude - of (0.07; 4) and (0.06; 6), respectively.
- Mixed phase (G and H): the addition of their respective profiles leads to $r_{max} = 0.03$ g kg$^{-1}$ at $z \approx 4$ km consistently to that GH observed one.
- Liquid phase (R and C): The R-class is mainly present below the 0°C isotherm with ($r_{max}$; $z$) = (0.08; 1) while the C-class dominates at $z = 2$ km with $r_{max} = 0.18$ g kg$^{-1}$ and is also present above the 0°C level (altitude of 3.5 km). That suggests the role of supercooled droplets in precipitation development.

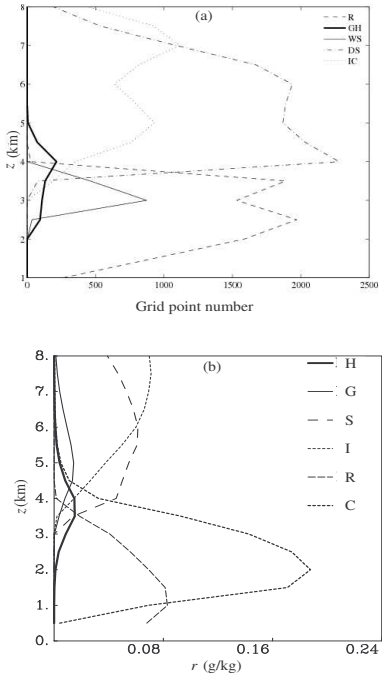


**Fig. 2.** (a) Vertical profile of the mean number of grid points associated with a hydrometeor class over the period 1700-2000 UTC. (b) Same as (a) but the profile is inferred form Meso-NH computations of hydrometeor mixing ratio $r$ (g kg$^{-1}$) in the box of figure 1b.

### 3.2 Temporal mean microphysical processes (Fig. 3)

In this subsection, budget Meso-NH computations are made to quantify the various microphysical processes considered as contributor to precipitation development. Precisely, the model gives the mixing ratio rate $\tau$ (µg kg$^{-1}$ s$^{-1}$) for a given duration. We have chosen the 1730 - 1930 UTC period because it corresponds to the most active phase of the system. Distinctions are made between the three phases (solid, mixed and liquid) and the processes are described in the following table.

Solid phase (Fig. 3a): DEPI and BRFI are the main contributors to I-formation with respective maximum coordinate ($\tau_{max}$, $z$) = (20; 8) and (5; 5). The non negligible presence of BRFI suggests consistently with Figure 2 the presence of supercooled droplets. In Meso-NH, the only way to initiate S is by AUTI which is very efficient at high altitudes. AGGS and RIMS are then responsible for S growth with ($\tau_{max}$, $z$) = (5; 5-8) and (15; 3.5); here also RIMS is an indicator of the role of supercooled water. For $z > 5$ km, RIMS is a sink: S is large enough [diameter of at least 7 mm (Farley et al 1989)] so that it is considered as G in Meso-NH.

Mixed phase (Fig. 3b): RIMG is the initiator of G and H when large aggregates interact with supercooled droplets or drops. Collection of others hydrometeors (I, S, C, R) in a wet or dry mode (GRWG) causes then G and H to grow. The former is such that ($\tau_{max}$, $z$) ≈ (12; 5) while for the latter

($\tau_{max}$, $z$) = (5; 4). Moreover, some G particles are turned into H (WTGH) which then can grow efficiently in the wet mode (WTHH) by collecting hydrometeors: ($\tau_{max}$, $z$) = (25; 4). Finally, CLMG [($\tau_{max}$, $z$) = (20; 3.5)] corresponds to the model to transformation of S falling through the melting layer in G; this kind of G can be associated to the WS category of Pujol et al. (2005).

Liquid phase (Fig. 3c): MLTR contributes to the increasing of R-amount with ($\tau_{max}$, $z$) = (20; 3.5). C are created by CNDC [($\tau_{max}$, $z$) = (20; 2] which is also present at negative temperatures ($z \approx 4.5$ km); that means that supercooled droplets are indeed present. R-formation is mainly due to warm coalescence AUTR + ACCR which are such that ($\tau_{max}$, $z$) = (5; 3) and ($\tau_{max}$, $z$) = (15; 2.5), respectively.

**Table.** Description of the different microphysical processes considered.

| Microphysical processes | | Definition |
|---|---|---|
| Solid phase | DEPI | Vapour deposition into ice (if positive) |
| | | Ice sublimation (if negative) |
| | BRFI | Wegener-Bergeron-Findeisen effect |
| | RIMS | Snow riming (if positive) |
| | | Turning of large aggregates into graupel (if negative) |
| | AGGS | Aggregation of ice crystals by snowflakes |
| | AUTI | Autoconversion of ice crystals into snow |
| Mixed phase | WTHH | Hail wet growth |
| | WTGH | Conversion of graupel growing in the wet mode into hail |
| | GRWG | Graupel dry and wet growths |
| | CMLG | Conversion of melting snow into melting graupel |
| | RIMG | Heavy riming of large aggregates converted into graupel |
| Liquid phase | CNDC | Condensation of vapour onto cloud droplets |
| | MLTR | Graupel and hail melting giving raindrops |
| | AUTR | Autoconversion of cloud droplets into raindrops |
| | ACCR | Accretion of cloud droplets by raindrops |

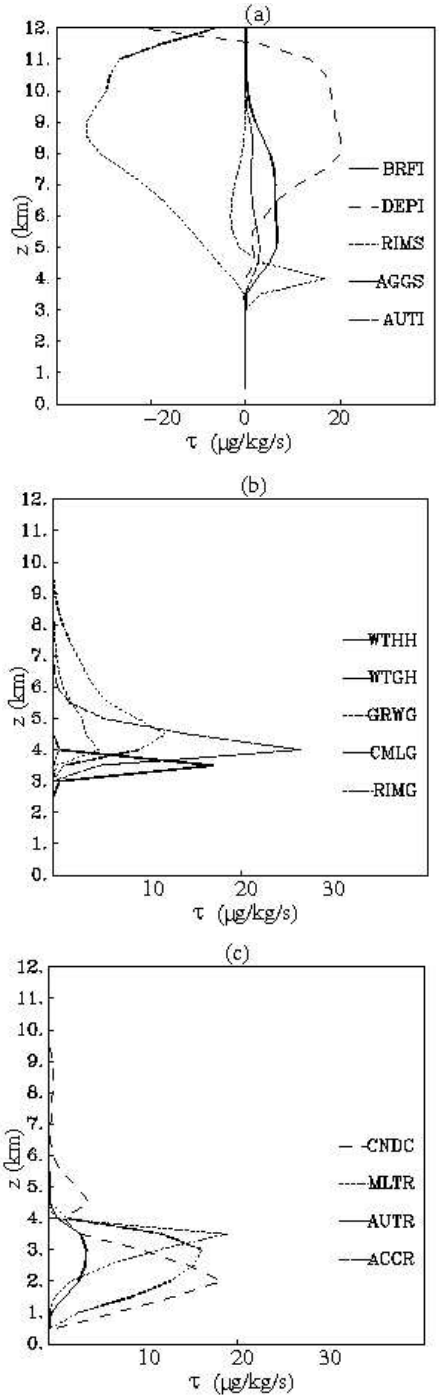


**Fig. 3.** Temporal mean vertical profile of the computed mixing ratio rates $\tau$ of the main microphysical processes. The same box and the same period than figure 2 are considered for computation.

To summarize, riming for snow development, heavy riming, wet growth and snow melting for graupel and hail development, as well as warm coalescence for rain appear to be efficient microphysical mechanisms with $\tau$-values close to 20 µg kg$^{-1}$ s$^{-1}$. Graupel fall and subsequent melting is an important contribution to rain enhancement at positive temperature with a same $\tau$-value. Vapour deposition and condensation for I- and C-formation are also characterized by the non negligible same $\tau$-values.

## 4 Conclusion

Radar and Meso-NH mean microphysical study are thus in agreement. Hydrometeor vertical profiles present similar pattern characteristic of microphysical convective processes. This study thus confirms and completes quantitatively the qualitative deduction from radar observations (Pujol et al. 2005) about the microphysical processes involved in orographic precipitation development. Particularly, the presence of supercooled water and the essential role of the ice phase are highlighted.

## References


Farley, R.D., P.E. Price, H.D. Orville, and J.H. Hirsch, 1989: On the numerical simulation of graupel/hail initiation via the riming of snow in bulk water microphysical cloud models. *J. Appl. Meteor.*, **28**, 1128-1131.

Keil, C. and C. Cardinali, 2004: The ECMWF Re-analysis of the Mesoscale Alpine Program Special Observing Period. *Q. J. R. Meteor. Soc.*, **130**, 2827-2850.

Lascaux, F., E. Richard, and J.P. Pinty, 2006: Numerical simulations of three different MAP IOPs and the associated microphysical processes. *Q. J. R. Meteor. Soc.*, in press.

Pujol, O., J.F. Georgis, M. Chong, and F. Roux, 2005: Dynamics and microphysics of orographic precipitation during MAP IOP3. *Q. J. R. Meteor. Soc.*, **131**, 2795-2819.